*Vietnam Journal of Science and Technology* ***57*** *(6) (2019) 762-772*

doi:10.15625/2525-2518/57/6/13905

# SIMULATION AND ANALYSIS OF A NOVEL MICRO-BEAM TYPE OF MEMS STRAIN SENSORS

**Nguyen Chi Cuong*, Trinh Xuan Thang, Tran Duy Hoai, Nguyen Thanh Phuong, Vu Le Thanh Long, Truong Huu Ly, Hoang Ba Cuong, Ngo Vo Ke Thanh**

*Research Laboratories of Saigon High-Tech-Park, Lot I3, N2 street, Saigon High-Tech-Park, District 9, Ho Chi Minh City*

*Email: *cuong.nguyenchi@shtplabs.org*

Received: 28 June 2019; Accepted for publication: 6 September 2019

**Abstract.** A new structure of a micro-strain beam type of Micro-Electro-Mechanical-Systems (MEMS) strain gauge is proposed and simulated. The stress and strain distributions of MEMS strain gauge are evaluated in x and y directions by 2D FEM simulation, respectively. The results showed that the longitudinal stress and strain distributions of strain beam enhance significantly, while the transverse stress and strain distributions are almost unchanged in the whole structure of MEMS strain gauge. High sensitivity of piezoresistive MEMS strain sensors can be designed to detect only one single direction of the stress and strain on the material objects.

*Keywords:* MEMS strain sensor, SHMS, piezoresistive, stress, strain.

*Classification numbers:* 2, 4, 5.

## 1. INTRODUCTION

The strain is one of the most important quantities to monitoring the health of infrastructures in Structural Health Monitoring Systems (SHMS) [1]. In order to measure the strain, the piezoresistive properties of electric materials for the strain measurement are used [2]. The conventional strain sensor is made by a very thin layer of metals such as Au [3], Cu [4], Mn [5], Au-glass [6], Bi-Sb [7], $RuO_2$ [8]. However, these metal foils strain sensors suffer from limited sensitivity, large temperature dependence, and high power consumption.

In order to improve the performance, Micro-Electro-Mechanical-Systems (MEMS) strain sensors can be fabricated using semiconductor materials such as silicon based on the MEMS technologies [9, 10]. MEMS strain sensors become more attractive due to high sensitivity, low noise, better scaling characteristics, low cost, and less complicated conditioning circuit [11]. Typically, MEMS strain gauges must be utilized to estimate both the magnitude and directions of stress or strain. Also, to improve the performance of MEMS strain gauge with greater sensitivity of strain measurements, MEMS strain gauge can be ideally used to measure stress or strain only in the longitudinal direction, and can't be affected by transverse movements for stress or strain of materials. Thus, many efforts have focused to design and fabricating higher sensitivity of piezoresistive MEMS strain sensors. Mohammed *et al*. [12] has proposed a better performance of strain sensors with creation of surface features (trenches) etched in vicinity of

sensing elements to create stress concentration regions. Also, Cao *et al*. [13] introduced a thin membrane served to amplify the strain in the wafer. Thus, strain sensitivity of these sensors are improved. However, a new structure of micro-strain beam type of MEMS strain sensors is not considered and designed yet.

In this study, a new design of micro-strain beam type of MEMS strain gauge is proposed and designed with a central micro-beam etched in vicinity of silicon wafer to amplify the strain on the wafer. A novel structure of the central strain beam is designed to improve the sensitivity of MEMS strain gauge by creating stress concentration regions. The stress and strain distributions of MEMS strain gauge are evaluated in *x* and *y* directions, respectively. Also, the longitudinal stress of strain beam of strain gauge is discussed in wide range of distributed tension loads and dimensions of strain beam to check the safe operation of MEMS strain gauge. Thus, a new structure of strain beam type of MEMS strain sensor can be applied to design higher sensitivity of piezoresistive MEMS strain sensors to detect only one single direction of the stress and strain on the material objects.

## 2. MATERIALS AND METHODS

### 2.1. Theoretical background for mechanical analysis system

In this theoretical analysis, the strain gauge problem can be oversimplified in order to understand the theoretical background and to identify the critical parameters for the device performance. To achieve this step, a simplified geometry of the strain beam of strain gauge can be considered in Figure 1 as below:

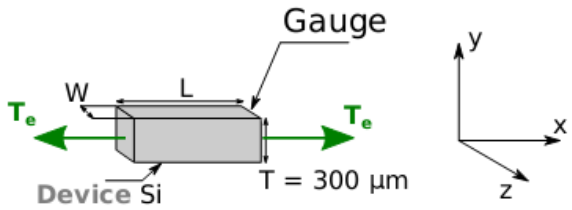


*Figure 1*. Simplified geometry of the strain beam of strain gauge used in theoretical background.

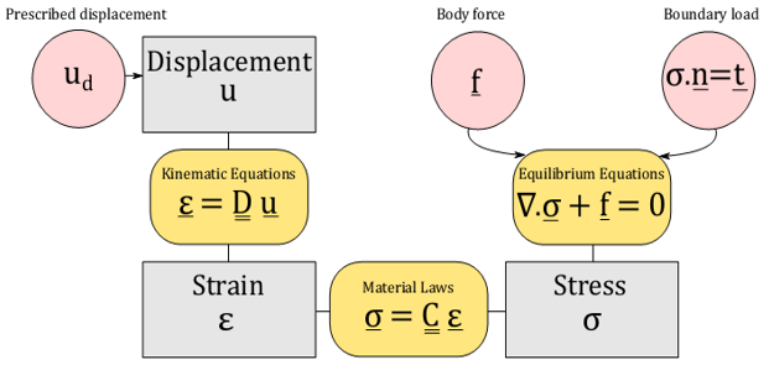


*Figure 2*. Fundamentals of mechanical analysis.

Let us assume that the slab of beam from Figure 1 is applied by a uniformly distributed load ($T_e$) over the thickness ($T$), and parallel to the middle plane, which is consistent with a plane

stress problem in the fundamental mechanical analysis [14]. In order to calculate the distributions of stress and strain in this elastic body subjected to a prescribed system of forces, several considerations regarding physical laws, material properties and geometry are required. These fundamentals are summarized in Figure 2.

In this figure, the outcomes (stress ($\sigma$), strain ($\varepsilon$), and displacement ($u$)) in the gray boxes depict the unknowns that need to solve in order to get all the desired knowledge about the mechanical system: The gray boxes are connected between each other through constitutive equations such as the kinematic equation, the material laws, and the equilibrium equation that need to be solved to get the quantities of interest of the stress and strain distributions [14].

*2.1.1. Stress-strain relations for homogeneous materials (material laws)*

Let us consider a linear elastic material behavior with orthotropic properties of homogeneous materials. In this theory, the external forces, which act on a solid body producing internal forces within the body interior and cause deformation or strain. The stresses applied to an infinitesimal portion of a solid body are described in Figure 3.

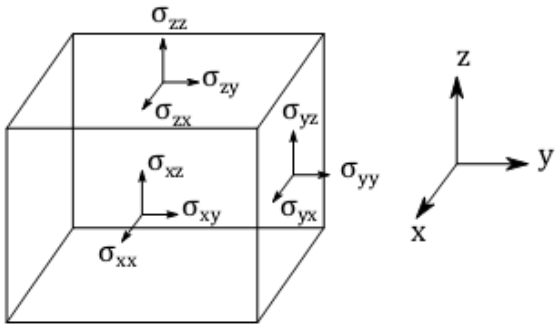


*Figure 3.* Stress components in a small cubic element of the material.

To relate stress and strain, we need to provide a material law. In the assumption of linear relations between stress and strain, we can write the general form of Hook's law:

$$\begin{bmatrix}\sigma_{xx}\\ \sigma_{yy}\\ \sigma_{zz}\\ \sigma_{yz}\\ \sigma_{xz}\\ \sigma_{xy}\end{bmatrix} = \underbrace{\hat{E}\begin{bmatrix} 1-\nu & \nu & \nu & 0 & 0 & 0\\ \nu & 1-\nu & \nu & 0 & 0 & 0\\ \nu & \nu & 1-\nu & 0 & 0 & 0\\ 0 & 0 & 0 & \frac{1-2\nu}{2} & 0 & 0\\ 0 & 0 & 0 & 0 & \frac{1-2\nu}{2} & 0\\ 0 & 0 & 0 & 0 & 0 & \frac{1-2\nu}{2}\end{bmatrix}}_{C}\begin{bmatrix}\varepsilon_{xx}\\ \varepsilon_{yy}\\ \varepsilon_{zz}\\ 2\varepsilon_{yz}\\ 2\varepsilon_{xz}\\ 2\varepsilon_{xy}\end{bmatrix} \tag{1}$$

where $\hat{E} = \dfrac{E}{(1+\nu)(1-2\nu)}$. Here, $E$ and $\nu$ are Young's modulus and Poisson' ratio, respectively. Furthermore, Eq. (1) can be reduced following the well-known plane stress assumptions: $\sigma_{xz} = \sigma_{yz} = \sigma_{zz} = 0$, then Eq. (1) becomes:

$$\begin{bmatrix} \sigma_{xx} \\ \sigma_{yy} \\ \sigma_{xy} \end{bmatrix} = \frac{E}{1-\nu^2} \begin{bmatrix} 1 & \nu & 0 \\ \nu & 1 & 0 \\ 0 & 0 & \frac{1-\nu}{2} \end{bmatrix} \begin{bmatrix} \varepsilon_{xx} \\ \varepsilon_{yy} \\ 2\varepsilon_{xy} \end{bmatrix} \tag{2}$$

Taking the inverse of Eq. (2) gives the strain as below:

$$\begin{bmatrix} \varepsilon_{xx} \\ \varepsilon_{yy} \\ 2\varepsilon_{xy} \end{bmatrix} = \frac{1}{E} \begin{bmatrix} 1 & -\nu & 0 \\ -\nu & 1 & 0 \\ 0 & 0 & 2(1+\nu) \end{bmatrix} \begin{bmatrix} \sigma_{xx} \\ \sigma_{yy} \\ \sigma_{xy} \end{bmatrix} \tag{3}$$

*2.1.2. Equations of equilibrium*

The equations of equilibrium in the *xy* -plane are given as follows:

$$\frac{\partial \sigma_{xx}}{\partial x} + \frac{\partial \sigma_{xy}}{\partial y} + f_x = 0 \tag{4}$$

$$\frac{\partial \sigma_{xy}}{\partial x} + \frac{\partial \sigma_{yy}}{\partial y} + f_y = 0 \tag{5}$$

where $f_x$ and $f_y$ are body force components along *x* and *y*-directions, respectively.

*2.1.3. Strain/displacement relations and compatibility of stress*

Let assume these symbols of *u*, *v*, and *w* are the displacement field components along *x*, *y* and *z* directions, respectively. The strain-displacement relations can be divided into two groups: the in-plane strain (*xy*-plane strain):

$$\varepsilon_{xx} = \frac{\partial u}{\partial x}, \quad \varepsilon_{yy} = \frac{\partial v}{\partial y}, \quad 2\varepsilon_{xy} = \left( \frac{\partial u}{\partial y} + \frac{\partial v}{\partial x} \right) \tag{6}$$

and the out-of-plane strain:

$$\varepsilon_{zz} = \frac{\partial w}{\partial z}, \quad 2\varepsilon_{xz} = \left( \frac{\partial u}{\partial z} + \frac{\partial w}{\partial x} \right), \quad 2\varepsilon_{yz} = \left( \frac{\partial v}{\partial z} + \frac{\partial w}{\partial y} \right) \tag{7}$$

Equation (5) can be rewritten in a single equation as called compatibility of strain and it is given by:

$$\frac{\partial^2 \varepsilon_{xx}}{\partial y^2} + \frac{\partial^2 \varepsilon_{yy}}{\partial x^2} = 2 \frac{\partial^2 \varepsilon_{xy}}{\partial x \partial y} = \frac{\partial^2 \gamma_{xy}}{\partial x \partial y} \tag{8}$$

Substituting Eq. (3) and using Eqs. (4, 5, 8), we can rewrite in order to obtain the compatibility of stress as follows:

$$\left( \frac{\partial^2}{\partial x^2} + \frac{\partial^2}{\partial y^2} \right) (\sigma_{xx} + \sigma_{yy}) = -(1+\nu) \left( \frac{\partial f_x}{\partial x} + \frac{\partial f_y}{\partial y} \right) \tag{9}$$

*2.1.4. Airy's stress function*

In the case of the body force components are negligible, the system of equation without boundary conditions can be summarized as follows:

$$\frac{\partial \sigma_{xx}}{\partial x} + \frac{\partial \sigma_{xy}}{\partial y} + f_x = 0, \qquad \frac{\partial \sigma_{xy}}{\partial x} + \frac{\partial \sigma_{yy}}{\partial y} + f_y = 0 \tag{10}$$

$$\left( \frac{\partial^2}{\partial x^2} + \frac{\partial^2}{\partial y^2} \right) (\sigma_{xx} + \sigma_{yy}) = 0 \tag{11}$$

The system of equations above is equally satisfied by the stress function, $\Phi(x,y)$ related to stresses as follows:

$$\sigma_{xx} = \frac{\partial^2 \Phi}{\partial y^2}, \qquad \sigma_{yy} = \frac{\partial^2 \Phi}{\partial x^2}, \qquad \sigma_{xy} = -\frac{\partial^2 \Phi}{\partial x \partial y} \tag{12}$$

substituting Eq. (12) into Eq. (11) gives:

$$\frac{\partial^4 \Phi}{\partial x^4} + 2\frac{\partial^4 \Phi}{\partial x^2 \partial y^2} + \frac{\partial^4 \Phi}{\partial y^4} = \nabla^4 \Phi = 0 \tag{13}$$

This is a formulation of a 2D-problem with no body force, that requires only a solution of the biharmonic equation in Eq. (13) and satisfy the boundary conditions (the applied tension load ($t$) and the clamped boundary). However, for a solution of a complex structure of MEMS strain gauge problem, the Finite Element Method must be required to simulate the proposed the 2D structure of MEMS strain gauge glued on a material object with some applied boundary conditions. After solving, the stress and strain distributions of MEMS strain gauge can be evaluated to measure/detect the change of the stress and strain on the material object.

### 2.2. 2D Finite element simulation

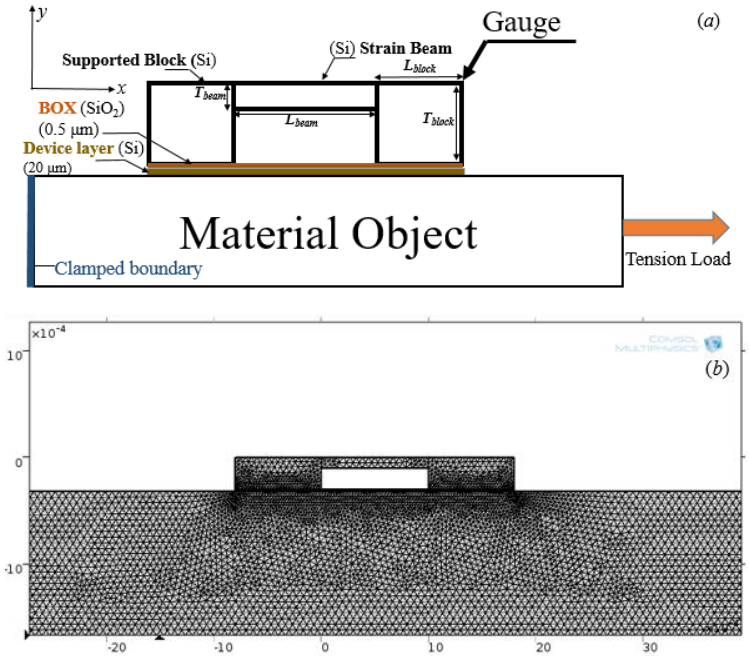


*Figure 4*. (a) 2D A cut view, (b) Mesh setting of the MEMS strain gauge simulated in COMSOL Multiphysics [15].

*Table 1*. The basic geometric and operating conditions of MEMS strain gauge used in COMSOL Multiphysics [15].

| Description | Name | Value |
|---|---|---|
| Beam length | $L_{beam}$ | 1000 μm |
| Beam width | $W_{beam}$ | 300 μm |
| Beam thickness | $T_{beam}$ | 100 μm |
| Applied tension load | $T_{input}$ | 50 MPa |
| Young's modulus of (100) Si [14] | $E_{Si}$ | 130 GPa |
| Poisson's ratio of (100) Si [14] | $v_{Si}$ | 0.28 |
| Density of materials of (100) Si [14] | $\rho_{Si}$ | 2330 kg/m$^3$ |
| Young's modulus of material object | $E_{object}$ | 200 GPa |
| Poisson's ratio of material object | $v_{object}$ | 0.3 |
| Density of materials of material object | $\rho_{object}$ | 7800 kg/m$^3$ |
| Elastic limit of Si | $\sigma_{limit}$ | 180 MPa |
| Strain limit of Si | $\varepsilon_{limit}$ | 1385 με |

In Figure 4 simulation, we proposed the 2D structure of MEMS strain gauge glued on a material object with the applied tensile load as showed in Figure 4 (a). A Silicon (Si) strain beam of MEMS strain gauge is supported between two blocks. Then, this structure of MEMS strain gauge (Si) with the BOX ($SiO_2$) and device layer (Si) are glued onto a material object. Boundary conditions are set with a tension load applied at one side and a clamped boundary applied at another side of material object. In Figure 4 (b), for mesh setting, we used a triangular mesh configuration with number of elements of 94851 for whole structure of MEMS strain gauge and the material object to yield acceptable convergence. Also, higher edge elements with number of 1553 are set for the edges between the strain beam, device layer, and blocks to ensure the correctness in 2D simulations of MEMS strain gauge. The dimension and operating conditions of a MEMS strain gauge are showed in the Table 1. Then, this structure is solved and simulated by the Structure Mechanics in the MEMS Modulus of the commercial COMSOL Multiphysics software [15]. After solving, the stress and strain distributions of MEMS strain gauge can be evaluated in *x* or *y* direction, respectively to measure/detect the change of the stress and strain on the material object.

## 3. RESULTS AND DISCUSSION

### 3.1. Stress and strain distributions of MEMS strain gauge

In this result, the stress and strain distributions of MEMS strain gauge are investigated in the *x* and *y* directions in wide range of the geometric and operating conditions. The basic geometric and operating conditions of strain gauge in Table 1 are utilized for this 2D FEM analysis. Thus, the stress and strain distributions of MEMS strain gauge can be obtained and discussed in *x* and *y* directions, respectively. Also, the longitudinal stress of strain beam of MEMS strain gauge is investigated in wide range of the distributed tension load ($T_e$) for various dimension (i.e. length ($L_{beam}$), width ($W_{beam}$), and thickness ($T_{beam}$)) of the strain beam to check

the safe operation of MEMS strain gauge. Finally, the obtained results can be applied to design for high sensitivity of MEMS strain sensors to detect the stress and strain generated on the material objects.

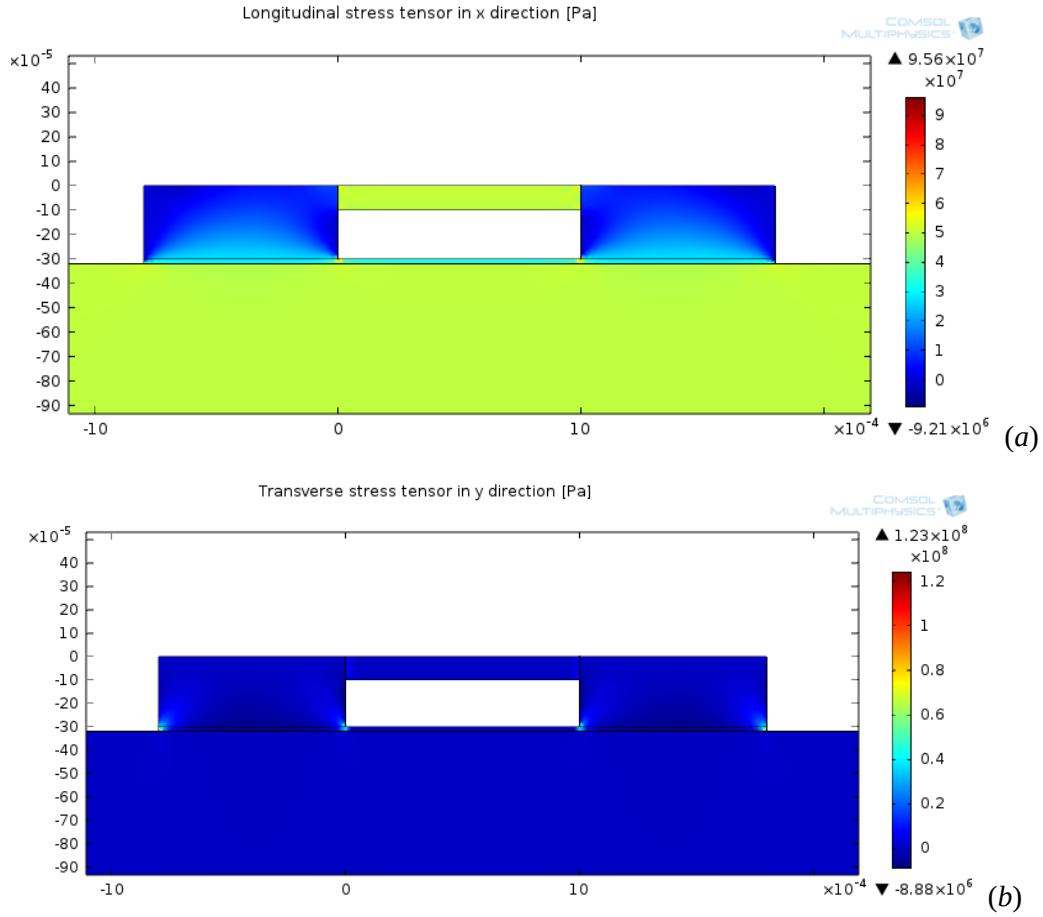


*Figure 5*. (a) Longitudinal stress distribution ($\sigma_{xx}$), (b) Transversal stress distribution ($\sigma_{yy}$) of MEMS strain gauge are plotted in 2D FEM domain.

In Figure 5 (*a*), the longitudinal stress distribution ($\sigma_{xx}$) in *x* direction is plotted in the 2D FEM domain of MEMS strain gauge. The results showed that $\sigma_{xx}$ becomes uniform and enhances considerably along strain beam of strain gauge. The corner places between the block and device layer also presented higher stress distributions than the other regions of strain gauge. Furthermore, the value of the stress ($\sigma_{xx}$) along the strain beam is obtained much higher than the other regions such as block, device layer, and material object. In Figure 5 (*b*), the transversal stress distribution ($\sigma_{yy}$) in *y* direction is plotted. The results showed that $\sigma_{yy}$ is almost unchanged along strain beam, block, device layer and material object. Higher $\sigma_{yy}$ is obtained at the corner places between the block and device layer. Thus, the longitudinal stress distribution ($\sigma_{xx}$) of strain beam is only amplified considerably in *x* direction, while the transverse stress distribution ($\sigma_{yy}$) of strain beam is almost unchanged in the whole structure of MEMS strain gauge.

In Figure 6(*a*), the longitudinal strain distribution ($\varepsilon_{xx}$) in *x* direction is plotted in the 2D FEM domain of MEMS strain gauge. The results showed that $\varepsilon_{xx}$ becomes uniform and enhances

significantly along the strain beam of MEMS strain gauge. The corner places between blocks and device layer also presented the high values of strain distribution. In Figure 6(*b*), the transversal strain distribution ($\varepsilon_{yy}$) in *y* direction is also plotted. The results showed that the value of $\varepsilon_{yy}$ is almost unchanged along strain beam, block, device layer, and material object. Thus, $\varepsilon_{xx}$ enhances significantly along the strain beam of strain gauge, while $\varepsilon_{yy}$ is almost unchanged in the whole of structure of MEMS strain gauge. Thus, the obtained results can be applied to design a high sensitivity of MEMS strain sensor to detect in only one single direction of the stress and strain generated in the material objects.

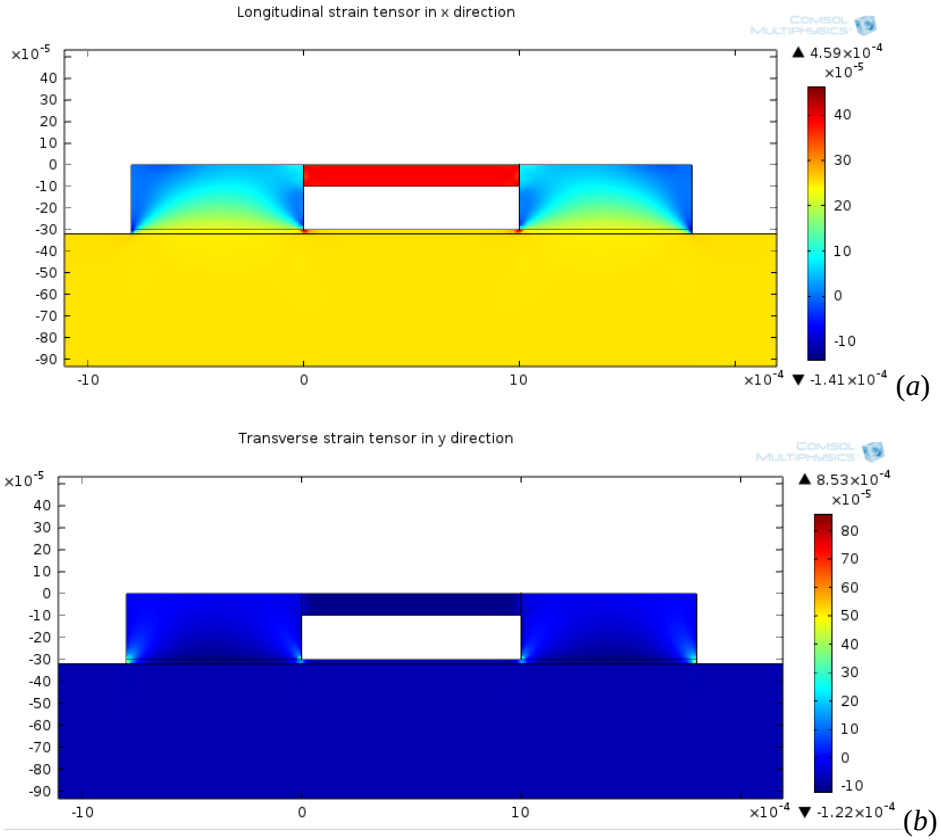


*Figure 6.* (*a*) The longitudinal strain ($\varepsilon_{xx}$), (*b*) the transversal strain ($\varepsilon_{yy}$) of MEMS strain gauge are plotted in 2D FEM domain.

Also, in Table 2, the present results of longitudinal strain ($\varepsilon_{xx}$) and transverse strain ($\varepsilon_{yy}$) are compared with the published data of some papers in the literature review. The results showed that the magnitudes of strain ($\varepsilon_{xx}$, $\varepsilon_{yy}$) of the present micro-strain beam structure of silicon strain gauge are almost higher than those published data of the other metallic and semiconductor strain gauges such as metallic thin foil [3], square or rectangular thin film [4, 5], semiconductor thin film with micro-groove or trench structures [12]. Thus, this new structure of MEMS strain gauge based on micro-strain beam type, which can be used to detect stress or strain on the material object in only one single direction, can be used to design a higher performance of piezoresistive MEMS strain sensors.

*Table 2.* Summary of longitudinal and transverse strain ($\varepsilon_{xx}$, $\varepsilon_{yy}$) of some metals and semiconductor strain sensors.

| **Authors** | **Types and Geometries** | **Materials** | **Maximum strain ($\varepsilon_{xx}$, $\varepsilon_{yy}$)** |
|---|---|---|---|
| Rajanna and Mohan [3] | thin foil sensors | metal: Au | $\varepsilon_{xx} \cong 230$ (με)<br>$\varepsilon_{yy} \cong 400$ (με) |
| Rajanna and Mohan [4, 5] | square or rectangular thin film sensors | metals: Cu, Mn | $\varepsilon_{xx} \cong 290$ - 370 (με)<br>$\varepsilon_{yy} \cong 270$ (με) |
| Mohammed et al. [12] | semiconductor thin film sensors with surface grove or trench structures | silicon | $\varepsilon_{xx} \cong 240$ (με) |
| The present study | semiconductor thin film sensors with micro-strain beam structures | silicon | $\varepsilon_{xx} \cong 459$ (με)<br>$\varepsilon_{yy} \cong 853$ (με) |

### 3.2. Effects of distributed tension load on the longitudinal stress ($\sigma_{xx}$)

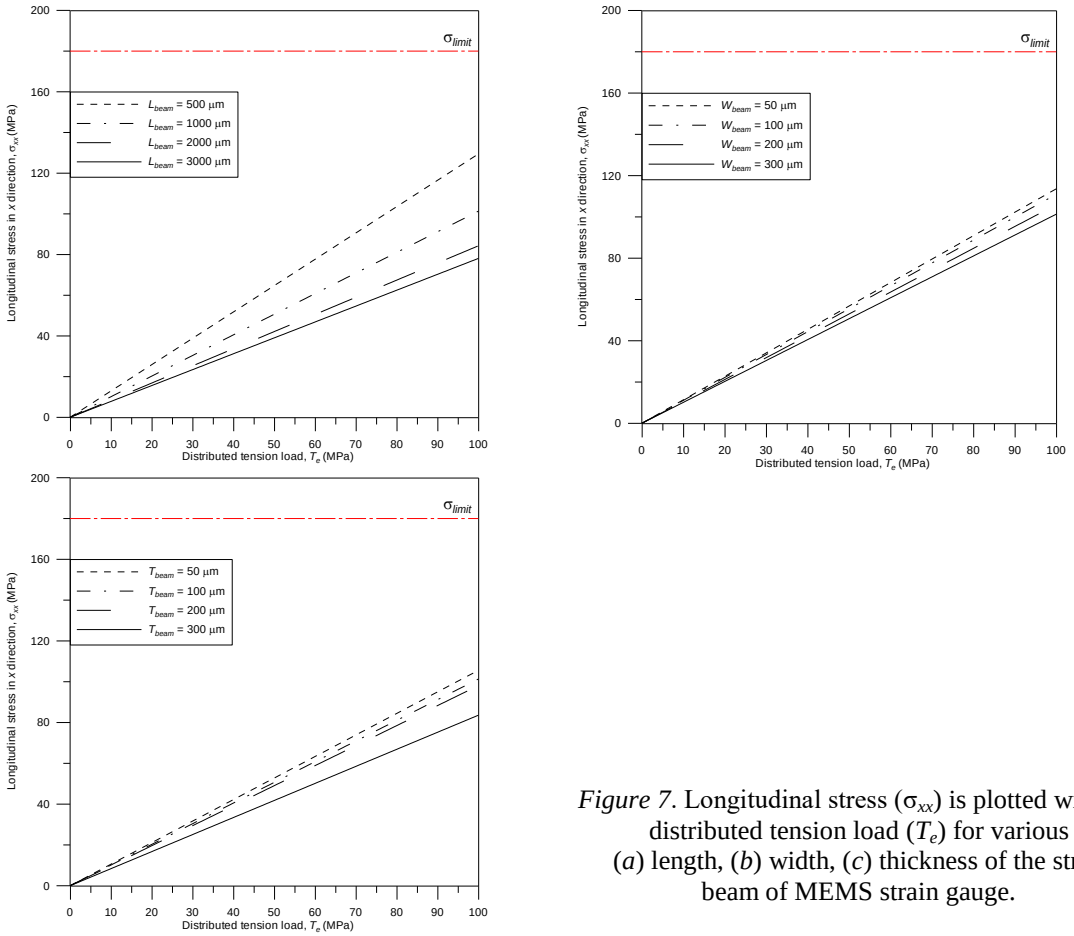


*Figure 7.* Longitudinal stress ($\sigma_{xx}$) is plotted with the distributed tension load ($T_e$) for various (*a*) length, (*b*) width, (*c*) thickness of the strain beam of MEMS strain gauge.

In Figure 7, the longitudinal stress ($\sigma_{xx}$) of the strain beam is plotted with the distributed tension load ($T_e$) for various length ($L_{beam}$), width ($W_{beam}$), and thickness ($T_{beam}$) of the strain beam of MEMS strain gauge. The elastic limit of silicon material ($\sigma_{limit}$ = 180 MPa) is used. Thus, the obtained results of stress distribution ($\sigma_{xx}$) must be smaller than these values of elastic limit ($\sigma_{limit}$) to ensure the strain gauge is safe enough to operate in wide range of the applied tension load ($T_e$). The results showed that $\sigma_{xx}$ increases significantly with $T_e$ in wide range of dimension of strain beam conditions. Also, the value of $\sigma_{xx}$ increases as $L_{beam}$ decreases as showed in Figure 7(*a*), $W_{beam}$ decreases as showed in Figure 7(*b*), and $T_{beam}$ decreases as showed in Figure 7(*c*). Furthermore, the value of $\varepsilon_{xx}$ does not beyond the value of elastic limit of silicon material ($\sigma_{limit}$ = 180 MPa) in wide range of distributed tension loads and dimensions of the strain beam. Thus, the MEMS strain gauge can be operated safely to avoid the break of strain gauge in wide range of the distributed tension loads and dimensions of strain beam of the MEMS strain gauge.

## 4. CONCLUSIONS

In this study, a new structure of micro-strain beam type of MEMS strain gauge is proposed and simulated by the 2D FEM in the COMSOL Multiphysics. MEMS strain gauge is designed with a central micro-strain beam etched in vicinity of silicon wafer to amplify the stress and strain on the material object. The stress and strain distributions of MEMS strain gauge are investigated in *x, y* directions, respectively. Also, the longitudinal stress of MEMS strain gauge is investigated over a wide range of distributed tension load and dimension of strain beam conditions. Some remarkable results are found as below:

1) The longitudinal stress/strain distributions of strain beam enhance significantly, while the transverse stress/strain distributions are almost unchanged in the whole structure of MEMS strain gauge. Thus, this new structure of MEMS strain gauge based on micro-strain beam type, which can be used to detect stress or strain on the material object in only one single direction, can be used to design a higher performance of piezoresistive MEMS strain sensors.
2) The longitudinal stress of the strain beam increases considerably with the distributed tension load. Also, the longitudinal stress of the strain beam increases as the length, width, and thickness of the strain beam decrease. The magnitudes of stress do not beyond the values of elastic limit of Si material in wide range of conditions. Thus, the MEMS strain gauge can be operated safely to avoid the break of strain gauge in wide range of the tension load and dimension conditions.

***Acknowledgements.*** This research was supported by the annual projects of The Research Laboratories of Saigon High Tech Park in 2019 according to decision No. 102/QĐ -KCNC of Management Board of Saigon High Tech Park and contract No. 01/2019/HĐNVTX-KCNC-TTRD (Project number 2).

## REFERENCES

1. Annamdas V. G. M., Bhalla S., and Soh C. K. - Applications of structural health monitoring technology in Asia, Structural Health Monitoring **16** (3) (2017) 324-346.
2. Mason W. P., and Thurston R. N. – Use of Piezoresistive materials in measuring displacement, force, and torque, J. Acoust. Soc. Am. **29** (1957) 1096-1101.

3. Rajanna K., and Mohan S. - Longitudinal and transverse strain sensitivity of gold film, J. Mater. Sci. Lett. **6** (1987) 1027-1029.
4. Rajanna K., and Mohan S. - Studies on meandering path thin film strain gage, Sensor. Actuat. A-Phys. **15** (1988) 297-303.
5. Rajanna K., and Mohan S. - Strain sensitive property of vacuum evaporated manganese films, Thin Solid Films **172** (1989) 45-50.
6. Witt G. R. – Some effects of strain and temperature on the resistance of thin gold-glass cermet films, Thin Solid Film **13** (1972) 109-115.
7. Sanpath S., and Ramanaiah V. - Behavior of Bi–Sb alloy thin films as strain gages, Thin Solid Films **137** (1986) 199–205.
8. Hrovat M., Holc J., and Samardzija Z. – The influence of firing temperature on gauge factors and the electrical and microstructural characteristics of thick-film resistor, J. Mater. Sci. Lett. **20** (2001) 701-705.
9. French P.J., and Evans A.G.R. - Polycrystalline silicon strain sensors, Sensor. Actuat. A-Phys. **8** (1985) 219–225.
10. Mohammed A. A. S., Moussa W. A., and Lou E. - Mechanical Strain Measurements Using Semiconductor Piezoresistive Material, The 2006 International Conference on MEMS, NANO and Smart Systems (2006) 5-6.
11. Fraden J. - Handbook of modern sensor: physics, designs, and applications, AIP Press-Springer: New York, 1996.
12. Mohammed A. A. S., Moussa W. A., and Lou E. - High-Performance Piezoresistive MEMS Strain Sensor with Low Thermal Sensitivity, Sensors **11** (2011) 1819-1846.
13. Cao L., Kim T. S., Mantell S. C., Mantell S. C., and Polla D. L. - Simulation and fabrication of piezoresistive membrane type MEMS strain sensors, Sensor. Actuat. A-Phys. **80** (2000) 273–279.
14. Bao M. - Analysis and Design Principles of MEMS Devices, Elsevier, 2005.
15. COMSOL 5.4 (2019) COMSOL Multiphysics.https://www.comsol. com/. June 4, 2019.